

growth along the dorso-ventral axis of the optic cup. *BMC Dev Biol* 2006;6:62.

11. Xie T, Liang J, Liu N, Huan C, Zhang Y, Liu W, *et al.* Transcription factor TBX4 regulates myofibroblast accumulation and lung fibrosis. *J Clin Invest* 2016;126:3063–3079.
12. Galambos C, Mullen MP, Shieh JT, Schwerk N, Kiehl MJ, Ullmann N, *et al.* Phenotype characterisation of *TBX4* mutation and deletion carriers with neonatal and paediatric pulmonary hypertension. *Eur Respir J* 2019;54:1801965.
13. Ruvinsky I, Oates AC, Silver LM, Ho RK. The evolution of paired appendages in vertebrates: T-box genes in the zebrafish. *Dev Genes Evol* 2000;210:82–91.
14. Morikawa M, Koinuma D, Tsutsumi S, Vasilaki E, Kanki Y, Heldin CH, *et al.* ChIP-seq reveals cell type-specific binding patterns of BMP-specific Smads and a novel binding motif. *Nucleic Acids Res* 2011;39:8712–8727.
15. Waldron L, Steimle JD, Greco TM, Gomez NC, Dorr KM, Kweon J, *et al.* The cardiac TBX5 interactome reveals a chromatin remodeling network essential for cardiac septation. *Dev Cell* 2016;36:262–275.

Copyright © 2021 by the American Thoracic Society



## **Mycoplasma pneumoniae-Specific IFN- $\gamma$ -Producing CD4<sup>+</sup> Effector-Memory T Cells Correlate with Pulmonary Disease**

To the Editor:

*Mycoplasma pneumoniae* (*Mp*) is a major cause of community-acquired pneumonia (CAP) in children (1). However, the pathogenesis of *Mp* CAP is not well understood. Lymphocyte responses against *Mp* have been reported to promote either protection or immunopathology in mice (1, 2). In humans, intradermal injection of *Mp* antigen elicited a delayed-type hypersensitivity skin reaction in patients with *Mp* infection (3). The size of the delayed-type hypersensitivity skin induration, which depends mainly on infiltrating CD4<sup>+</sup> T helper 1 (Th1) cells, correlated with the severity of pulmonary infiltrates in those patients (3). These observations suggest that the *Mp*-specific T-cell response contributes to *Mp* pulmonary disease.

We showed that the measurement of specific IgM antibody-secreting cells (ASCs) in blood discriminated patients with CAP with *Mp* infection from *Mp* carriers suffering from CAP caused by other pathogens (4). Using this well-diagnosed cohort, we here investigated the *Mp*-specific T-cell response and its contribution to pulmonary disease.

Ⓜ This letter is open access and distributed under the terms of the Creative Commons Attribution Non-Commercial No Derivatives License 4.0 (<http://creativecommons.org/licenses/by-nc-nd/4.0/>). For commercial usage and reprints, please contact Diane Gern ([dgern@thoracic.org](mailto:dgern@thoracic.org)).

Supported by a Walter und Gertrud Siegenthaler Fellowship and the career development program "Filling the Gap" of the University of Zurich (P.M.M.S.). The funder had no role in the study design, data collection and analysis, decision to publish, or preparation of the manuscript.

Author Contributions: Conception and design: E.P., W.W.J.U., and P.M.M.S. Analysis and interpretation: E.P., W.W.J.U., C.B., and P.M.M.S. Drafting the manuscript for important intellectual content: W.W.J.U. and P.M.M.S.

This letter has a data supplement, which is accessible from this issue's table of contents at [www.atsjournals.org](http://www.atsjournals.org).

Children with CAP ( $n = 35$ ) and healthy controls (HCs;  $n = 16$ ) aged 3–18 years from a prospective longitudinal study (4, 5) from which peripheral blood mononuclear cells (PBMCs) were available were included in this study. Baseline characteristics of subjects are shown in Table E1 in the data supplement. The study was approved by the ethics committee of Zurich, Switzerland (no. 2016-00148). Detailed methods are shown in the data supplement. CAP disease severity was assessed based on chest radiograph (CXR) findings, hypoxemia (oxygen saturation as measured by pulse oximetry  $< 93\%$ ) requiring oxygen supply, and inflammatory parameters (6). CXRs were graded with an adapted CXR severity scoring system (7), with grades 1, 2, and 3 representing increasing severity (Table E2 and Figure E1).

We first developed an *Mp*-specific IFN- $\gamma$  enzyme-linked immunospot (ELISpot) assay (data supplement (5, 8)) and demonstrated its specificity by comparing patients with *Mp* PCR-positive ( $Mp^+$ ) CAP and  $Mp^+$  HCs (carriers), as well as patients with *Mp* PCR-negative ( $Mp^-$ ) CAP and  $Mp^-$  HCs (Figure 1A). The ELISpot assay detected IFN- $\gamma$  released by PBMCs after stimulation with *Mp* antigen most frequently and pronounced in patients with  $Mp^+$  CAP (Figures 1A and 1B). This is in line with IgM ASC ELISpot assay results, which confirmed *Mp* infection in those patients with  $Mp^+$  CAP (Table E1). However, in contrast to IgM ASCs, which were short lived (5) and mainly present during the symptomatic stage ( $\leq 20$  days after onset of symptoms), the *Mp*-specific IFN- $\gamma$  response was significantly longer lasting and also detectable in the convalescent stage ( $> 20$  days) ( $P = 0.0007$ ) (Figure 1C).

To identify the IFN- $\gamma$ -producing cells, we depleted CD4<sup>+</sup> or CD8<sup>+</sup> T cells from PBMCs of a patient with  $Mp^+$  CAP (Figure E2). Depletion of CD4<sup>+</sup> T cells reduced IFN- $\gamma$  spot-forming units (SFUs) by 96% and 88% upon 24 hours and 48 hours preincubation with *Mp* antigen, respectively (Figure 1D). CD8 depletion did not markedly reduce IFN- $\gamma$  SFUs. These findings were corroborated by flow cytometry: only IFN- $\gamma$ -producing CD4<sup>+</sup> T cells, and almost no CD8<sup>+</sup> T cells, were detected (Figure 1E). Among these IFN- $\gamma$ -producing CD4<sup>+</sup> T cells, a significant proportion coexpressed CD69 and CD40L, identifying antigen-responsive T cells (data not shown). Importantly, the majority of IFN- $\gamma^+$ CD4<sup>+</sup> T cells were detected in the effector-memory T cell ( $T_{EM}$ ) compartment (Figures 1F and E3).

Th1 cells have been reported to contribute to immune-mediated tissue damage in other infectious diseases (9–14). Therefore, we correlated the *Mp*-specific IFN- $\gamma$  response with disease severity in  $Mp^+$  CAP (Table E3). The extent of pulmonary disease reflected by increased CXR grading correlated positively with the degree of the specific IFN- $\gamma$  response in symptomatic ( $R = 0.49$ ,  $P = 0.03$ ) and convalescent stage ( $R = 0.62$ ,  $P = 0.006$ ) (Figures 1G and 1H). Interestingly, in contrast to patients with CXR grade 1, those with CXR grades 2 and 3 showed even an increase in IFN- $\gamma$ -producing cells over time (Figure 1I). The IFN- $\gamma$  response was antigen dose dependent and most pronounced for patients with CXR grade 3 (Figures 1J and E4A). However, the IFN- $\gamma$  response did not correlate with bacterial load in the upper respiratory tract. No relation was observed between CXR grading and bacterial load (Figure E4B) or the *Mp*-specific B-cell response (Figure E5). The acute IFN- $\gamma$  response was also associated with C-reactive protein levels ( $P = 0.009$ ; Figure 1K) and oxygen need

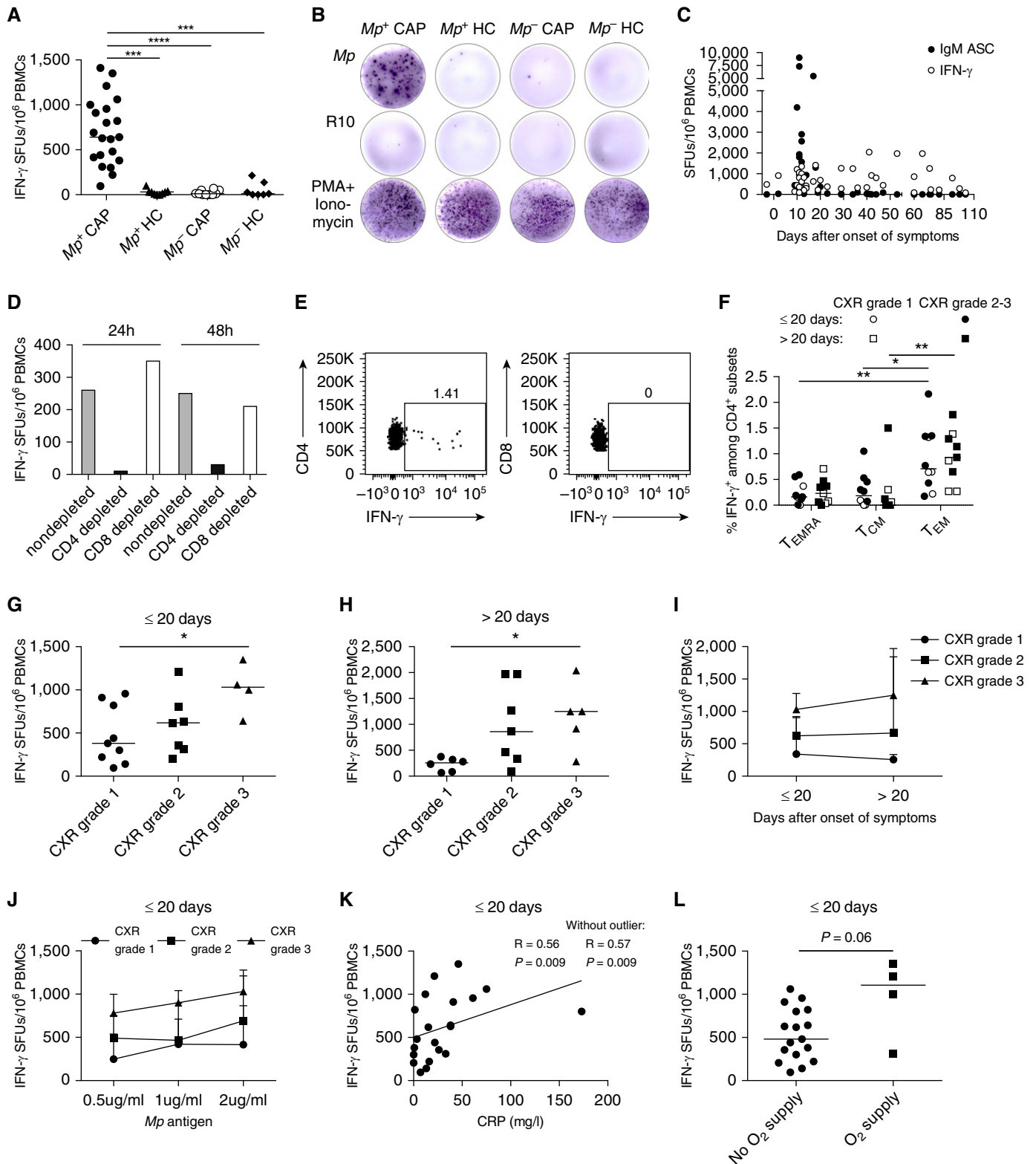


**Figure 1.** *Mp*-specific IFN- $\gamma$  response by CD4 $^+$  T cells. (A and B) *Mp*-specific IFN- $\gamma$  SFUs per  $10^6$  PBMCs (A) and representative patterns (B) in ELISpot assay of *Mp* $^+$  CAP ( $n=21$  of the total 25 patient samples in Table E1 [ $n=1$  exclusively used for flow cytometry in E and F;  $n=3$  only available at the convalescent stage]; samples collected at median 12 days [interquartile range, 11–16] after symptom onset), *Mp* $^+$  HC (carrier,  $n=9$ ), *Mp* $^-$  CAP ( $n=10$ ),

( $P = 0.06$ ; Figure 1L). In contrast to the IFN- $\gamma$  response (Figure 1I), C-reactive protein returned to normal levels in all patients at the convalescent stage (Figure E4C).

To our knowledge, these are the first data indicating that CD4<sup>+</sup> T<sub>EM</sub> cells form the major population of the pathogen-specific IFN- $\gamma$  response in children with *Mp* CAP, and that the presence of these Th1 cells in peripheral blood correlates with pulmonary disease severity.

The IFN- $\gamma$  ELISpot assay is one of the most sensitive *ex vivo* detection methods for pathogen-specific T cells (8). Here, we demonstrate high specificity of the *Mp*-specific IFN- $\gamma$  ELISpot assay in a well-diagnosed cohort of patients with CAP and healthy controls (4, 5). Interestingly, the detection of the IFN- $\gamma$  response by ELISpot assay allowed also a differentiation between *Mp* infection and carriage. However, in contrast to the IgM ASC response, which is short-lived and associated with clinical disease (5), the long-lasting nature of the *Mp*-specific IFN- $\gamma$  response may pose a limitation to the IFN- $\gamma$  ELISpot assay as diagnostic test for *Mp* infection.

Our findings on the *Mp*-specific Th1 cell response are corroborated by previous observations in animal models suggesting that Th1 cells contribute to inflammatory lesions in mycoplasma pneumonia (1, 2, 15), and clinical studies in children and adults where the IFN- $\gamma$  response correlated with the disease severity and/or radiological changes in CAP associated with *Mp* (16–18). Furthermore, we expand these observations by revealing *Mp*-specific T<sub>EM</sub> cells as the major Th1 cell compartment associated with more severe disease. In fact, Th1-mediated immunopathology has been proposed to play a role in other infectious diseases (9–14). T<sub>EM</sub> cells migrate to inflamed peripheral tissues and display immediate effector function (19, 20). The higher INF- $\gamma$  response in patients with *Mp* CAP with severe disease, which even increased over time despite bacterial clearance, points to dysregulation and expansion of effector-memory Th1 cells rather than to a more pronounced or persistent triggering by *Mp* antigens.

In conclusion, these data further support the hypothesis that host cell-mediated immunity, particularly pathogen-specific IFN- $\gamma$ -producing CD4<sup>+</sup> T<sub>EM</sub> cells, is involved in the pathogenesis of *Mp* CAP. Further studies are required to reveal the exact role of these cells in *Mp* pulmonary disease. ■

**Author disclosures** are available with the text of this letter at [www.atsjournals.org](http://www.atsjournals.org).

**Acknowledgment:** The authors thank the children and their parents who contributed to this study; the emergency department staff, the division of anesthesiology staff, the division of otolaryngology staff, the outpatient clinic staff, and the short-stay department staff (University Children's Hospital Zurich) for recruiting participants; the microbiology laboratory staff (University Children's Hospital Zurich) for processing samples; Martin Hersberger (Division of Clinical Chemistry and Biochemistry, University Children's Hospital Zurich) for conducting the C-reactive protein analyses; and the primary care physicians and pediatricians for participating in out-of-hospital follow-up visits.

Elena Pánisová, Ph.D.\*  
University Children's Hospital Zurich  
Zurich, Switzerland

Wendy W. J. Unger, Ph.D.\*  
Erasmus MC University Medical Center–Sophia Children's Hospital  
Rotterdam, the Netherlands

Christoph Berger, M.D.  
Patrick M. Meyer Sauter, M.D., Ph.D.†  
University Children's Hospital Zurich  
Zurich, Switzerland

ORCID IDs: 0000-0002-8489-8406 (E.P.); 0000-0001-9484-261X (W.W.J.U.); 0000-0002-2373-8804 (C.B.); 0000-0002-4312-9803 (P.M.M.S.).

\*These authors contributed equally to this work.

†Corresponding author (e-mail: [patrick.meyer@kispi.uzh.ch](mailto:patrick.meyer@kispi.uzh.ch)).

**Figure 1.** (Continued). and *Mp*<sup>-</sup> HC ( $n = 7$ ) (100,000 PBMCs per well). (C) *Mp*-specific IgM ASC (filled symbols) or IFN- $\gamma$  (empty symbols) SFUs per 10<sup>6</sup> PBMCs by ELISpot assay in relation to days after onset of symptoms ( $n = 41$  *Mp*<sup>+</sup> CAP patient samples;  $n = 21$  during symptomatic stage [ $\leq 20$  days after onset of symptoms] and  $n = 20$  in convalescent stage [ $> 20$  days after onset of symptoms]). (D) IFN- $\gamma$  SFUs per 10<sup>6</sup> PBMCs (ELISpot assay) of a patient with *Mp*<sup>+</sup> CAP without depletion (gray bars) or with depletion of CD4<sup>+</sup> (black bars) and CD8<sup>+</sup> (white bars) T cells. PBMCs were preincubated for 24 hours and 48 hours with *Mp* antigen. (E) Representative flow cytometry dot plots of *Mp*-specific CD4<sup>+</sup>IFN- $\gamma$ <sup>+</sup> and CD8<sup>+</sup>IFN- $\gamma$ <sup>+</sup> T<sub>EM</sub> cells of a patient with *Mp*<sup>+</sup> CAP at the symptomatic stage. The percentages of IFN- $\gamma$ <sup>+</sup> cells are indicated. (F) IFN- $\gamma$ -producing memory CD4<sup>+</sup> T-cell subsets measured by flow cytometry of patients with *Mp*<sup>+</sup> CAP during symptomatic stage ( $\leq 20$  d,  $n = 10$ ; circles) and convalescent stage ( $> 20$  d,  $n = 9$ ; squares), and in relation to CXR grade 1 (white symbols) and grade 2–3 (black symbols). CD4<sup>+</sup> T-cell subsets were stained with antibodies binding to CD45RA and CCR7 (T<sub>EMRA</sub>: CD45RA<sup>+</sup>CCR7<sup>-</sup>; T<sub>CM</sub>: CD45RA<sup>-</sup>CCR7<sup>+</sup>; T<sub>EM</sub>: CD45RA<sup>-</sup>CCR7<sup>-</sup>). There were no statistically significant differences between percentage of IFN- $\gamma$ <sup>+</sup> cells and CXR grading per subset and stage of disease. (G–I) *Mp*-specific IFN- $\gamma$  SFUs per 10<sup>6</sup> PBMCs of patients with *Mp*<sup>+</sup> CAP in relation to CXR grading (grades 1, 2, and 3 represent increasing severity) during symptomatic stage ( $\leq 20$  d) ( $n = 20$  of the 21 patients in A–C with acute sample and also CXR available) (G), convalescent stage ( $> 20$  d) ( $n = 18$  of the 20 patients in C with convalescent sample and also CXR available) (H), and over time ( $n = 16$  patients with both acute and convalescent sample and also CXR available) (I). (J) IFN- $\gamma$  response upon prestimulation for 24 hours with 0.5  $\mu$ g/ml, 1  $\mu$ g/ml, and 2  $\mu$ g/ml antigen during symptomatic stage ( $\leq 20$  d) from patients with CXR grade 1 ( $n = 7$ ), grade 2 ( $n = 6$ ), and grade 3 ( $n = 4$ ). (K and L) *Mp*-specific IFN- $\gamma$  SFUs per 10<sup>6</sup> PBMCs of patients with *Mp*<sup>+</sup> CAP ( $n = 21$ ), preincubated with 2  $\mu$ g/ml of *Mp* antigen for 24 hours, and assessed on the basis of CRP levels (K) or need for oxygen supply (L) during symptomatic stage ( $\leq 20$  d). Horizontal lines (A, F–H, and L) or symbols (I and J) indicate median values and whiskers extend to the first and third quartile. Statistical significance was determined by Kruskal-Wallis test with *post hoc* Dunn's multiple comparisons test (A and F–J), Mann-Whitney U test (L), or Spearman rank correlation (K). The CXR grades (1–2–3) were used as numerical values for statistical analysis. \* $P < 0.05$ , \*\* $P < 0.01$ , \*\*\* $P < 0.001$ , and \*\*\*\* $P < 0.0001$ ; only statistically significant differences are indicated in the graphs. ASC = antibody-secreting cell; CAP = community-acquired pneumonia; CRP = C-reactive protein; CXR = chest radiograph; HC = healthy control; *Mp* = *Mycoplasma pneumoniae*; PBMC = peripheral blood mononuclear cell; R10 = complete RPMI; SFU = spot-forming unit; T<sub>CM</sub> = central-memory T cell; T<sub>EM</sub> = effector-memory T cell; T<sub>EMRA</sub> = terminally differentiated effector-memory T cell.

## References

1. Waites KB, Talkington DF. *Mycoplasma pneumoniae* and its role as a human pathogen. *Clin Microbiol Rev* 2004;17:697–728.
2. Jones HP, Tabor L, Sun X, Woolard MD, Simecka JW. Depletion of CD8<sup>+</sup> T cells exacerbates CD4<sup>+</sup> Th cell-associated inflammatory lesions during murine mycoplasma respiratory disease. *J Immunol* 2002;168:3493–3501.
3. Mizutani H, Kitayama T, Hayakawa A, Nagayama E. Delayed hypersensitivity in *Mycoplasma pneumoniae* infections. *Lancet* 1971; 1:186–187.
4. Meyer Sauteur PM, Seiler M, Trück J, Unger WWJ, Paioni P, Rely C, et al. Diagnosis of *Mycoplasma pneumoniae* pneumonia with measurement of specific antibody-secreting cells. *Am J Respir Crit Care Med* 2019;200:1066–1069.
5. Meyer Sauteur PM, Trück J, van Rossum AMC, Berger C. Circulating antibody-secreting cell response during *Mycoplasma pneumoniae* childhood pneumonia. *J Infect Dis* 2020;222:136–147.
6. Bradley JS, Byington CL, Shah SS, Alverson B, Carter ER, Harrison C, et al.; Pediatric Infectious Diseases Society and the Infectious Diseases Society of America. The management of community-acquired pneumonia in infants and children older than 3 months of age: clinical practice guidelines by the Pediatric Infectious Diseases Society and the Infectious Diseases Society of America. *Clin Infect Dis* 2011;53:e25–e76.
7. Taylor E, Haven K, Reed P, Bissielo A, Harvey D, McArthur C, et al.; SHIVERS Investigation Team. A chest radiograph scoring system in patients with severe acute respiratory infection: a validation study. *BMC Med Imaging* 2015;15:61.
8. Streeck H, Frahm N, Walker BD. The role of IFN-gamma Elispot assay in HIV vaccine research. *Nat Protoc* 2009;4:461–469.
9. Silveira-Mattos PS, Narendran G, Akrami K, Fukutani KF, Anbalagan S, Nayak K, et al. Differential expression of CXCR3 and CCR6 on CD4<sup>+</sup> T-lymphocytes with distinct memory phenotypes characterizes tuberculosis-associated immune reconstitution inflammatory syndrome. *Sci Rep* 2019;9:1502.
10. Findlay EG, Greig R, Stumhofer JS, Hafalla JC, de Souza JB, Saris CJ, et al. Essential role for IL-27 receptor signaling in prevention of Th1-mediated immunopathology during malaria infection. *J Immunol* 2010;185:2482–2492.
11. Liu G, Xu J, Wu H, Sun D, Zhang X, Zhu X, et al. IL-27 signaling is crucial for survival of mice infected with African Trypanosomes via preventing lethal effects of CD4<sup>+</sup> T cells and IFN- $\gamma$ . *PLoS Pathog* 2015;11:e1005065.
12. de Oliveira Mendes-Aguiar C, Vieira-Gonçalves R, Guimarães LH, de Oliveira-Neto MP, Carvalho EM, Da-Cruz AM. Effector memory CD4<sup>+</sup> T cells differentially express activation associated molecules depending on the duration of American cutaneous leishmaniasis lesions. *Clin Exp Immunol* 2016;185:202–209.
13. Ohta A, Sekimoto M, Sato M, Koda T, Nishimura S, Iwakura Y, et al. Indispensable role for TNF-alpha and IFN-gamma at the effector phase of liver injury mediated by Th1 cells specific to hepatitis B virus surface antigen. *J Immunol* 2000;165:956–961.
14. Eaton KA, Benson LH, Haeger J, Gray BM. Role of transcription factor T-bet expression by CD4<sup>+</sup> cells in gastritis due to *Helicobacter pylori* in mice. *Infect Immun* 2006;74:4673–4684.
15. Fonseca-Aten M, Ríos AM, Mejías A, Chávez-Bueno S, Katz K, Gómez AM, et al. *Mycoplasma pneumoniae* induces host-dependent pulmonary inflammation and airway obstruction in mice. *Am J Respir Cell Mol Biol* 2005;32:201–210.
16. Tanaka H, Koba H, Honma S, Sugaya F, Abe S. Relationships between radiological pattern and cell-mediated immune response in *Mycoplasma pneumoniae* pneumonia. *Eur Respir J* 1996;9: 669–672.
17. Tanaka H, Narita M, Teramoto S, Saikai T, Oashi K, Igarashi T, et al. Role of interleukin-18 and T-helper type 1 cytokines in the development of *Mycoplasma pneumoniae* pneumonia in adults. *Chest* 2002;121:1493–1497.
18. Yang M, Meng F, Gao M, Cheng G, Wang X. Cytokine signatures associate with disease severity in children with *Mycoplasma pneumoniae* pneumonia. *Sci Rep* 2019;9:17853.
19. Luettig B, Kaiser M, Bode U, Bell EB, Sparshott SM, Bette M, et al. Naive and memory T cells migrate in comparable numbers through the normal rat lung: only effector T cells accumulate and proliferate in the lamina propria of the bronchi. *Am J Respir Cell Mol Biol* 2001;25: 69–77.
20. Walrath J, Zukowski L, Krywiak A, Silver RF. Resident Th1-like effector memory cells in pulmonary recall responses to *Mycobacterium tuberculosis*. *Am J Respir Cell Mol Biol* 2005;33:48–55.

Copyright © 2021 by the American Thoracic Society



### Lung Gene Expression Analysis Web Portal Version 3: Lung-at-a-Glance

To the Editor:

Recent advances in single-cell omics have provided increasing insights into the pathogenesis of human diseases, including those affecting the lung (1–7). The density of omics data relevant to lung biology and diseases is increasing exponentially through the work of research consortia and individual investigators (1, 3, 8–12). Discerning the best way to optimize the use of these rich datasets, integrate multiomics data, extract biologically meaningful knowledge, and make that knowledge available to the research community in a user-friendly manner is a challenging opportunity. With support from the National Heart, Lung, and Blood Institute (NHLBI) “LungMAP” (Lung Map) consortium, we developed the Lung Gene Expression Analysis (LGEA) database and web portal to facilitate access and visualization of extensive bulk, sorted, single-cell transcriptomic and image data from human and mouse lungs at different stages of development and disease (13, 14). Data hosted on LGEA are primarily produced by LungMAP research centers. We process and interpret the data and make it available to all investigators before its publication (8). LGEA has been widely used by researchers from more than 130 institutions from 52 different countries and has been cited in more than 130 scientific publications. The newly updated LGEA version 3 introduces a new featured web toolset, “lung-at-a-glance,” for exploring and understanding complex multiomics and imaging data, providing an interactive web interface to bridge lung anatomic ontology classifications to lung structure, histology, and immunofluorescence confocal images and cell type-specific gene expression.

Lung-at-a-glance consists of “region,” “cell,” and “gene,” three interactive components all designed to provide data access with a single click on the icons ([https://research.cchmc.org/pbge/lunggens/tools/lung\\_at\\_glance.html](https://research.cchmc.org/pbge/lunggens/tools/lung_at_glance.html)). We name the toolset as

Supported by U.S. National Institutes of Health grants U01HL122642, U01HL148856, U01HL134745, and P30 DK117467 and the Chan Zuckerberg Foundation (Human Cell Atlas Lung Seed Network).

Author Contributions: Y.D., M.G., and Y.X. conceived and designed the web application. Y.D. developed the database and web application of Lung Gene Expression Analysis web portal. W.O. developed the web application of Lung Gene Expression Analysis lung ontology. Y.D. and W.O. developed the lung-at-a-glance toolsets. J.A.K. and J.A.W. designed and developed the web application of lung image. Y.D., M.G., S.Z., and Y.X. contributed to data analysis and interpretation. Y.D., J.A.W., and Y.X. wrote the manuscript. All authors contributed to the manuscript editing and approved the final manuscript.

This letter has a data supplement, which is accessible from this issue’s table of contents at [www.atsjournals.org](http://www.atsjournals.org).